

Energy-superconvergent Runge-Kutta Time Discretizations

Jinjie Liu^{*} and Moysey Brio[†]

May 10, 2024

Abstract

In this paper, we investigate the energy accuracy of explicit Runge-Kutta (RK) time discretization for antisymmetric autonomous linear systems and present a framework for constructing RK methods with an order of energy accuracy much greater than the number of stages. For an s -stage, p th-order RK method, we show that the energy accuracy can achieve superconvergence with an order up to $2s - p + 1$ if p is even. Several energy-superconvergent methods, including five- to seven-stage fourth-order methods with energy accuracy up to the eleventh order, together with their strong stability criteria, are derived. The proposed methods are examined using several applications, including second-order ordinary differential equations for harmonic oscillators, linear integro-differential equations for peridynamics, and one-dimensional Maxwell's equations of electrodynamics.

Keywords: Runge-Kutta methods; Superconvergence; Hamiltonian; Energy accuracy; Peridynamics; Maxwell's equations.

MSC: 65L06, 65M12, 35Q61, 74A70

1 Introduction

Runge-Kutta (RK) algorithms are popular time discretization methods for solving systems of ordinary differential equations (ODEs) and ODE systems obtained from semi-discretized partial differential equations (PDEs). Besides stability and convergence rate of the solution, energy accuracy is another important property to consider when choosing RK methods, especially for energy conserving systems. Generally, only implicit RK methods can preserve the energy, but this requires solving a large system of equations. In contrast, explicit RK methods are more efficient but not energy-preserving. Energy can also be used to analyze stability and to achieve strong stability [1, 2, 3, 4, 5, 6, 7].

In this paper, we investigate the energy accuracy of explicit RK methods for antisymmetric linear autonomous systems. Some typical applications of antisymmetric linear autonomous systems include Hamiltonian systems, semi-discretized Maxwell's equations, and linear peridynamic nonlocal PDEs [8]. The energy accuracy of linear autonomous systems has been studied in [6], where it was shown that the energy order is at least $p + 1$ for a method of even order p . For an s -stage method, the energy equation is a polynomial of degree $2s$ in terms of the time step h . Therefore, the maximum order of energy accuracy is $2s - 1$, provided all coefficients vanish except the highest-order one. Setting all coefficients to zero results in an overdetermined system, so generally there is no solution. However, for antisymmetric systems, all the odd-order terms vanish, leading to a solvable system. Based on the solution, we are able to derive a class of energy-superconvergent RK methods, where the order of energy accuracy is greater than the

^{*}Division of Physics, Engineering, Mathematics, and Computer Science, Delaware State University, Dover, DE 19901 USA. jliu@desu.edu.

[†]Department of Mathematics, The University of Arizona, Tucson, AZ 85721 USA. brio@math.arizona.edu.

number of stages. For an s -stage method of even order p , the energy accuracy can achieve up to an order of $2s - p + 1$. For example, we construct a 7-stage fourth-order method with an energy order of 11. Furthermore, we derive the strongly stable fourth-order RK methods and their corresponding stability criteria. The proposed energy-superconvergent methods are tested using several one-dimensional examples, including second-order ODEs for harmonic oscillators, integro-differential equations for linear peridynamic models, and Maxwell's equations of electrodynamics.

The paper is organized as follows: In Section 2, we present the energy accuracy analysis that leads to the proposed energy-superconvergent methods. One-dimensional numerical examples are provided in Section 3, covering second-order ODEs for harmonic oscillators in Section 3.1, linear integro-differential equations in Section 3.2, and Maxwell's equations in Section 3.3, followed by the conclusion in Section 4.

2 Energy-superconvergent time discretization

We consider the autonomous linear ordinary differential equation (ODE) system:

$$\frac{d}{dt}u = Lu, \quad (1)$$

where L is antisymmetric, i.e., $L^T H + HL = 0$ for some symmetric and positive definite matrix H . The total energy (Hamiltonian) of this system is given by:

$$\mathcal{E} = \frac{1}{2}\|u\|_H^2 = \frac{1}{2}\langle u, u \rangle_H. \quad (2)$$

Here, $\langle \cdot, \cdot \rangle_H$ represents the H -inner product, defined by $\langle x, y \rangle_H = \langle x, Hy \rangle$ where $\langle \cdot, \cdot \rangle$ is the Euclidean inner product. $\|\cdot\|_H$ is the corresponding H -norm. In this section, we drop the subscript H and simply write $\|\cdot\| = \|\cdot\|_H$.

A general s -stage RK time discretization for the system (1) can be written as:

$$u_{n+1} = G_s u_n, \quad (3)$$

where

$$G_s = \sum_{k=0}^s a_k (hL)^k, \quad a_0 = 1, \quad a_s \neq 0. \quad (4)$$

Here h is the time step and $\{a_k\}_{k=0}^s$ are method dependent coefficients. The method is of order p if the first $p + 1$ terms in G_s coincide with the p th Taylor polynomial of e^{hL} .

Since $L^T H + HL = 0$, we have ([6], Corollary 2.2)

$$\langle L^i u, L^j u \rangle_H = \begin{cases} (-1)^{(j-i)/2} \|L^{(i+j)/2} u\|^2, & i + j \text{ is even,} \\ 0, & i + j \text{ is odd,} \end{cases} \quad (5)$$

and the energy equation

$$\mathcal{E}_{n+1} = \mathcal{E}_n + \frac{1}{2} \sum_{k=1}^s b_k h^{2k} \|L^k u_n\|^2, \quad (6)$$

where

$$b_k = \sum_{i=\max(0, 2k-s)}^{\min(2k, s)} (-1)^{k+i} a_i a_{2k-i} = a_k^2 + 2 \sum_{i=1}^{\min(k, s-k)} (-1)^i a_{k-i} a_{k+i}, \quad (7)$$

and \mathcal{E}_n and \mathcal{E}_{n+1} represent the energy at two consecutive times. Let m be the leading index of equation (6), i.e., $b_m \neq 0$ and $b_k = 0$ for all $1 \leq k < m$. Then the leading coefficient is b_m and the order of energy accuracy is $r = 2m - 1$. In this paper, we use s , p , and r to represent the number of stages, the order of the solution accuracy, and the order of energy accuracy,

respectively. An s -stage, p th-order method with r -th order of energy accuracy is denoted by $\text{RK}(s,p,r)$.

The Proposition 4.7 in [6] reveals that $r = p$ if p is odd, and $r \geq p + 1$ if p is even. When p is even and $p = s$, using the binomial theorem

$$\sum_{i=0}^k \frac{(-1)^i}{i!(k-i)!} = 0, \quad (8)$$

we can calculate the leading coefficient as follows:

$$b_{s/2+1} = (-1)^{s/2+1} \sum_{i=2}^s (-1)^i \cdot \frac{1}{i!} \cdot \frac{1}{(s+2-i)!}, \quad (9)$$

$$= (-1)^{s/2+1} \left(\sum_{i=0}^{s+2} \frac{(-1)^i}{i!(s+2-i)!} - \frac{-2}{(s+1)!} - \frac{2}{(s+2)!} \right), \quad (10)$$

$$= (-1)^{s/2+1} \left(\frac{2}{(s+1)!} - \frac{2}{(s+2)!} \right) \neq 0, \quad (11)$$

so $r = s + 1$. We summarize this result in the following proposition.

Proposition 1. *For an s -stage Runge-Kutta method of order $p = s$ applied to system (1), the order of energy accuracy is $r = 2\lfloor s/2 \rfloor + 1$, i.e., $r = s$ if s is odd and $r = s + 1$ if s is even.*

For instance, if $p = s = 4$, then $a_1 = 1$, $a_2 = 1/2$, $a_3 = 1/6$, $a_4 = 1/24$, $b_1 = b_2 = 0$, $b_3 = -1/72$, and $b_4 = 1/576$. This leads to

$$\mathcal{E}_{n+1} = \mathcal{E}_n - \frac{1}{72}h^6 \|L^3 u_n\|^2 + \frac{1}{576}h^8 \|L^4 u_n\|^2 = \mathcal{E}_n + \mathcal{O}(h^6), \quad (12)$$

and therefore $r = 5$. In [5], Corollary 2.1 proves that this four-stage fourth-order RK method is strongly stable if $h\|L\| \leq 2\sqrt{2}$, where $\|L\|$ is the matrix norm: $\|L\| = \sup_{\|v\|=1} \|Lv\|$. A more general result is given in the following lemma.

Lemma 1. *An s -stage RK method applied to system (1) is strongly stable if:*

- (i) $b_k = 0$ for $1 \leq k \leq s - 2$,
- (ii) $b_{s-1} < 0$, and
- (iii)

$$h\|L\| \leq \sqrt{\frac{-b_{s-1}}{b_s}}. \quad (13)$$

Proof. Because of condition (i), the energy equation (6) becomes:

$$\mathcal{E}_{n+1} = \mathcal{E}_n + \frac{1}{2}b_{s-1}h^{2s-2} \|L^{s-1}u\|^2 + \frac{1}{2}b_s h^{2s} \|L^s u\|^2, \quad (14)$$

where $b_s = a_s^2 > 0$. Condition (ii) and (iii) imply that:

$$b_s h^2 \|L\|^2 \leq -b_{s-1}, \quad (15)$$

and thus

$$\mathcal{E}_{n+1} - \mathcal{E}_n = \frac{1}{2}(b_{s-1} + b_s h^2 \|L\|^2) h^{2s-2} \|L^{s-1}u\|^2 \leq 0. \quad (16)$$

Therefore, the method is strongly stable. \square

When $p < s$ and p is an even number, there are $s - p$ free parameters: $\{a_k\}_{k=p+1}^s$. If they form a solution to the system of the same number of equations $b_k = 0$ for $p/2 + 1 \leq k \leq s - p/2$, then the leading index is $s - p/2 + 1$ and the order of energy accuracy is $r = 2s - p + 1$. Therefore, we have the following proposition.

Proposition 2. For an s -stage RK method of order p applied to system (1), if p is even, then $p + 1 \leq r \leq 2s - p + 1$.

When p is even and $s = p + 1$ or $s = p + 2$, we can derive the expressions of the coefficients $\{a_k\}$ in the following two propositions.

Proposition 3. If $s > 1$ is odd, and the coefficients of an s -stage method applied to the system (1) satisfy the following conditions:

$$a_k = \frac{1}{k!}, \quad k = 1, 2, \dots, s - 1, \quad (17)$$

$$a_s = \frac{1}{s!} - \frac{1}{(s + 1)!}, \quad (18)$$

then $p = s - 1$ and $r = s + 2$.

Proposition 4. If $s > 4$ is even, and the coefficients of an s -stage method applied to the system (1) satisfy the following conditions:

$$a_k = \frac{1}{k!}, \quad k = 1, 2, \dots, s - 2, \quad (19)$$

$$a_{s-1} = \frac{3}{(s + 2)!} - \frac{3}{(s + 1)!} + \frac{1}{(s - 1)!}, \quad (20)$$

$$a_s = \frac{3}{(s + 2)!} - \frac{3}{(s + 1)!} + \frac{1}{s!}, \quad (21)$$

then $p = s - 2$ and $r = s + 3$.

According to Propostion 2, when $p = 2$, an s -stage method achieves the best energy accuracy $r = 2s - 1$ if the set of coefficients $\{a_k\}_{k=3}^s$ forms a solution to the system of equations: $b_k = 0$ for $2 \leq k \leq s - 1$. For $3 \leq s \leq 5$, the coefficients are listed in Table 1, and the stability regions of these second-order methods and a fourth-order method are shown in Figure 1. The RK(4,4,5) method is the classical fourth-order RK method, known as the RK4. Most methods have comparable or larger stability regions than the RK4, except RK(4,2,7)-b and RK(5,2,9)-b.

Table 1: Coefficients and the corresponding orders of accuracy when $p = 2$.

method	s	p	r	a_1	a_2	a_3	a_4	a_5
RK(3,2,5)	3	2	5	1	$\frac{1}{2}$	$\frac{1}{8}$	-	-
RK(4,2,7)-a	4	2	7	1	$\frac{1}{2}$	$\frac{2-\sqrt{2}}{4}$	$\frac{3-2\sqrt{2}}{8}$	-
RK(4,2,7)-b	4	2	7	1	$\frac{1}{2}$	$\frac{2+\sqrt{2}}{4}$	$\frac{3+2\sqrt{2}}{8}$	-
RK(5,2,9)-a	5	2	9	1	$\frac{1}{2}$	$\frac{\sqrt{5}-1}{8}$	$\frac{\sqrt{5}-2}{8}$	$\frac{(\sqrt{5}-2)^2}{16(\sqrt{5}-1)}$
RK(5,2,9)-b	5	2	9	1	$\frac{1}{2}$	$\frac{1}{4}$	$\frac{1}{8}$	$\frac{1}{32}$

When $p = 2$, the leading coefficient $b_s = a_s^2 > 0$, and the method is not strongly stable [6]. To obtain strongly stable methods, we consider $p = 4$, where the energy accuracy can reach an order of $r = 2s - 3$, given that there exists a solution to the system of equations $b_k = 0$ for

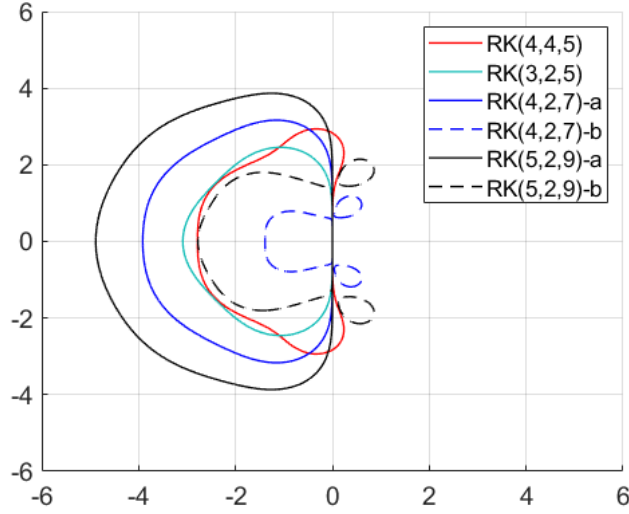


Figure 1: Stability regions of several second-order methods and the RK(4,4,5) method.

$3 \leq k \leq s - 2$. For example, when $s = 7$ we get

$$b_1 = a_1^2 - 2a_0a_2, \quad (22)$$

$$b_2 = a_2^2 - 2a_1a_3 + 2a_0a_4, \quad (23)$$

$$b_3 = a_3^2 - 2a_2a_4 + 2a_1a_5 - 2a_0a_6, \quad (24)$$

$$b_4 = a_4^2 - 2a_3a_5 + 2a_2a_6 - 2a_1a_7, \quad (25)$$

$$b_5 = a_5^2 - 2a_4a_6 + 2a_3a_7, \quad (26)$$

$$b_6 = a_6^2 - 2a_5a_7, \quad (27)$$

$$b_7 = a_7^2. \quad (28)$$

If $p = 4$, then $a_1 = 1$, $a_2 = 1/2$, $a_3 = 1/6$, $a_4 = 1/24$, and $b_1 = b_2 = 0$. Thus, by setting $b_3 = b_4 = b_5 = 0$, we obtain a system of three equations with three unknowns a_5 , a_6 , and a_7 :

$$\begin{cases} 2a_5 - 2a_6 - \frac{1}{72} = 0, \\ -\frac{1}{3}a_5 + a_6 - 2a_7 + \frac{1}{576} = 0, \\ a_5^2 - \frac{1}{12}a_6 + \frac{1}{3}a_7 = 0. \end{cases} \quad (29)$$

System (29) has one positive solution: $a_5 = \frac{\sqrt{10}-2}{144}$, $a_6 = \frac{\sqrt{10}-3}{144}$, and $a_7 = \frac{8\sqrt{10}-25}{3456}$. Furthermore, in this case, we can verify that the leading coefficient $b_6 = \frac{\sqrt{9604}-\sqrt{9610}}{248832} < 0$, so the method is strongly stable, as Theorem 2.7 in [6] has proven that a negative leading coefficient implies strong stability. Similarly, we can calculate the coefficients and verify the strong stability for $s = 5$ and $s = 6$. Additionally, we can find the strong stability criterion using Lemma 1 and it is summarized in the following theorem.

Theorem 1. *For an s -stage, fourth-order RK method applied to system (1), if the coefficients $\{a_k\}_{k=3}^s$ form a solution to the system of equations $b_k = 0$ for $3 \leq k \leq s - 2$, and $b_{s-1} = a_{s-1}^2 - 2a_s a_{s-2} < 0$, then the order of energy accuracy is $r = 2s - 3$. Furthermore, the method is strongly stable if*

$$h\|L\| \leq \lambda = \sqrt{\frac{2a_s a_{s-2} - a_{s-1}^2}{a_s^2}}. \quad (30)$$

Table 2 lists the coefficients of four- to seven-stage methods of order four and the corresponding λ values in the strong stability criterion (30). Only coefficients with indices larger than p

are listed, as $a_k = 1/k!$ if $k \leq p$. Additionally, the stability regions are illustrated in Figure 2. It demonstrates that as s increases, the stability region expands.

Table 2: Coefficients and stability criteria of fourth-order RK methods for $4 \leq s \leq 7$.

method	s	p	r	a_5	a_6	a_7	b_{s-1}	λ
RK(4,4,5)	4	4	5	-	-	-	$-\frac{1}{72}$	$2\sqrt{2}$
RK(5,4,7)	5	4	7	$\frac{1}{144}$	-	-	$-\frac{1}{1728}$	$2\sqrt{3}$
RK(6,4,9)	6	4	9	$\frac{1}{128}$	$\frac{1}{1152}$	-	$-\frac{5}{442368}$	$\sqrt{15}$
RK(7,4,11)	7	4	11	$\frac{\sqrt{10}-2}{144}$	$\frac{\sqrt{10}-3}{144}$	$\frac{8\sqrt{10}-25}{3456}$	$-\frac{\sqrt{9610}-\sqrt{9604}}{248832}$	$4\sqrt{\frac{3(31\sqrt{10}-98)}{5(253-80\sqrt{10})}} \approx 4.06$

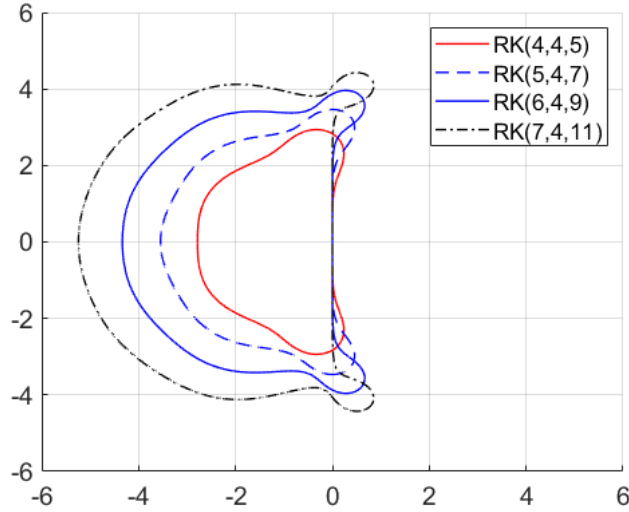


Figure 2: Stability regions of several fourth-order methods.

Because the order of energy accuracy exceeds that of both the solution and the number of stages, we refer to it as the energy superconvergence phenomenon, and we term the corresponding RK method the energy-superconvergent RK (ESC-RK) method.

To construct an s -stage RK method using the coefficients $\{a_k\}$, we can use the following algorithm:

$$\begin{aligned}
 k_0 &= 0, \\
 k_j &= c_j h L(u_n + k_{j-1}), \quad j = 1, 2, \dots, s, \\
 u_{n+1} &= u_n + k_s,
 \end{aligned} \tag{31}$$

where

$$c_j = \frac{a_{s-j+1}}{a_{s-j}}, \quad j = 1, 2, \dots, s. \tag{32}$$

3 Examples

In this section, various ODE systems are simulated using the proposed methods, including second-order ODEs for harmonic oscillators, one-dimensional integro-differential equation for

peridynamics, and the ODE systems derived from the semi-discretized one-dimensional Maxwell's equations of electrodynamics.

The convergence of the solution is measured using standard L_1 , L_2 , and L_∞ error norms, denoted by ϵ_1 , ϵ_2 , and ϵ_∞ , respectively. To test the energy accuracy, we calculate the convergence rate of the relative energy deviation:

$$\epsilon_E = \frac{\mathcal{E}_T - \mathcal{E}_0}{\mathcal{E}_0}, \quad (33)$$

where \mathcal{E}_0 and \mathcal{E}_T represent the energy at the initial and the final times, respectively.

3.1 Second-order differential equation for harmonic oscillator

In the first example, we consider the second-order differential equation for a harmonic oscillator:

$$\begin{aligned} x''(t) + a^2x(t) &= 0, \quad 0 \leq t \leq T, \\ x(0) = x_0, \quad x'(0) &= v_0. \end{aligned} \quad (34)$$

This equation can be written in matrix form as:

$$\frac{d}{dt}u = \begin{pmatrix} 0 & 1 \\ -a^2 & 0 \end{pmatrix}u, \quad (35)$$

where $u = \begin{pmatrix} x \\ v \end{pmatrix}$ and $v(t) = x'(t)$. The total energy of this system is given by:

$$\mathcal{E} = \frac{1}{2}\langle u, u \rangle_H = \frac{1}{2}(a^2x^2 + v^2), \quad (36)$$

where $H = \begin{pmatrix} a^2 & 0 \\ 0 & 1 \end{pmatrix}$.

In our simulations, we set $a = 1$, $T = 80$, $x_0 = 1$, and $v_0 = 0$. The exact solution is $x(t) = x_0 \cos(at)$. We use a uniform time step $\Delta t = T/N_t$ for all methods, where N_t represents the number of grid points.

Table 3 presents the results obtained from several second-order RK methods, with coefficients provided in Table 1, along with the Störmer–Verlet (SV) method [9]. We adopt RK(4,2,7)-a and RK(5,2,9)-a due to their larger stability regions compared to their corresponding b-versions. These results illustrate the convergence rates of these methods, including their orders of energy accuracy. Notably, when $N_t = 1600$, the relative energy deviation of RK(5,2,9) achieves machine precision ($\sim 10^{-16}$). Regarding the solution accuracy, the RK(3,2,5) has similar accuracy to the SV method, and as s increases, the errors decrease. For this set of second-order RK methods, the relative energy deviations are positive, indicating that these methods are not strongly stable.

The results of fourth-order methods are presented in Table 4. Similar to the second-order methods, the errors decrease as s increases. However, unlike the second-order methods, the relative energy deviations are all negative, indicating strong stability. We compare the performance of various fourth-order methods, as illustrated in Table 5. In this test, the 7-stage method exhibits better computational efficiency than the 4-stage method as it achieves a smaller error with a coarser mesh ($N_t/2$). It's worth noting that the 7-stage method has a larger step size limit (refer to Table 2), so better efficiency can be achieved if we use a larger Δt .

To assess energy dissipation, we conduct long time simulations ($T = 1000$) with $N_t = 5000$. Figure 3 illustrates the time history plots of the magnitude of relative energy deviations for the fourth-order methods, along with the corresponding linear fitting lines. The slope of the fitting lines decrease by several orders of magnitude as s increases by one, indicating a significant improvement in energy accuracy when superconvergent methods are used.

Table 3: Solution and energy convergence rates of harmonic oscillator simulations using several second-order RK methods.

Method	N_t	ϵ_1	Order	ϵ_2	Order	ϵ_∞	Order	ϵ_E	Order
SV	100	6.62E-01		8.30E-02		1.77E+00		-5.43E-02	
	200	1.74E-01	1.93	1.57E-02	2.40	5.30E-01	1.74	-3.30E-02	0.72
	400	4.28E-02	2.02	2.74E-03	2.52	1.34E-01	1.99	-9.99E-03	1.72
	800	1.06E-02	2.01	4.82E-04	2.51	3.32E-02	2.01	-2.49E-03	2.01
	1600	2.65E-03	2.00	8.50E-05	2.50	8.29E-03	2.00	-6.18E-04	2.01
RK(3,2,5)	100	7.54E-01		9.49E-02		2.02E+00		5.05E-01	
	200	1.79E-01	2.08	1.62E-02	2.55	5.46E-01	1.89	1.29E-02	5.29
	400	4.31E-02	2.05	2.76E-03	2.55	1.35E-01	2.02	4.00E-04	5.01
	800	1.06E-02	2.02	4.83E-04	2.52	3.33E-02	2.02	1.25E-05	5.00
	1600	2.65E-03	2.00	8.50E-05	2.50	8.29E-03	2.00	3.91E-07	5.00
RK(4,2,7)-a	100	3.49E-01		4.45E-02		9.70E-01		7.75E-03	
	200	8.41E-02	2.05	7.63E-03	2.54	2.62E-01	1.89	6.03E-05	7.01
	400	2.07E-02	2.02	1.33E-03	2.52	6.47E-02	2.02	4.71E-07	7.00
	800	5.16E-03	2.01	2.34E-04	2.51	1.61E-02	2.01	3.68E-09	7.00
	1600	1.29E-03	2.00	4.12E-05	2.50	4.02E-03	2.00	2.87E-11	7.00
RK(5,2,9)-a	100	2.05E-01		2.64E-02		6.17E-01		8.53E-05	
	200	5.03E-02	2.03	4.56E-03	2.53	1.57E-01	1.98	1.67E-07	9.00
	400	1.24E-02	2.01	7.97E-04	2.51	3.88E-02	2.01	3.25E-10	9.00
	800	3.10E-03	2.01	1.40E-04	2.51	9.68E-03	2.00	6.31E-13	9.01
	1600	7.74E-04	2.00	2.48E-05	2.50	2.42E-03	2.00	$\sim 10^{-16}$	-

3.2 Linear peridynamic integro-differential equation

The theory of peridynamics [8] can be employed to model the nonlocal wave interaction of a homogeneous and infinitely long bar. The governing equation is a one-dimensional nonlocal integro-differential equation, which in the linear case, can be written as

$$\rho(x)u_{tt}(x, t) = \int_{-\infty}^{\infty} C(\tilde{x} - x)(u(\tilde{x}, t) - u(x, t))d\tilde{x} + b(x, t), \quad (37)$$

where u , ρ , b , and C represent the displacement field, the density, the external force, and the micromodulus function, respectively. In this test, we utilize a normal distribution for the micromodulus function

$$C(x) = \begin{cases} \frac{4}{\sqrt{\pi}}e^{-x^2}, & |x| < \delta, \\ 0, & \text{otherwise,} \end{cases} \quad (38)$$

where $\delta > 0$ represents the horizon. To discretize equation (37), we partition the domain $[a, b]$ into N_x cells and define x_i at the cell centers: $x_i = a + (j - 1/2)\Delta x$, $j = 1, 2, \dots, N_x$, where $\Delta x = (b - a)/N_x$. The integral in equation (37) can be approximated using the midpoint quadrature method:

$$\int_{-\infty}^{\infty} C(\tilde{x} - x_i)(u(\tilde{x}, t) - u(x_i, t))d\tilde{x} \approx \sum_{j=1}^{N_x} C(x_j - x_i)(u_j - u_i)\Delta x. \quad (39)$$

Table 4: Solution and energy convergence rates of harmonic oscillator simulations using several fourth-order RK methods.

Method	N_t	ϵ_1	Order	ϵ_2	Order	ϵ_∞	Order	ϵ_E	Order
RK(4,4,5)	100	8.24E-02		1.04E-02		2.40E-01		-2.85E-01	
	200	5.43E-03	3.92	4.90E-04	4.41	1.63E-02	3.88	-1.11E-02	4.68
	400	3.39E-04	4.00	2.17E-05	4.50	1.03E-03	3.99	-3.54E-04	4.97
	800	2.12E-05	4.00	9.61E-07	4.50	6.54E-05	3.97	-1.11E-05	4.99
	1600	1.32E-06	4.00	4.24E-08	4.50	4.12E-06	3.99	-3.47E-07	5.00
RK(5,4,7)	100	1.78E-02		2.26E-03		5.34E-02		-9.15E-03	
	200	9.62E-04	4.21	8.71E-05	4.70	2.98E-03	4.16	-7.48E-05	6.93
	400	5.75E-05	4.06	3.69E-06	4.56	1.79E-04	4.06	-5.91E-07	6.99
	800	3.55E-06	4.02	1.61E-07	4.52	1.11E-05	4.01	-4.63E-09	7.00
	1600	2.21E-07	4.01	7.09E-09	4.51	6.91E-07	4.00	-3.62E-11	7.00
RK(6,4,9)	100	6.01E-03		7.66E-04		1.84E-02		-1.16E-04	
	200	3.49E-04	4.11	3.16E-05	4.60	1.08E-03	4.09	-2.35E-07	8.95
	400	2.14E-05	4.03	1.37E-06	4.53	6.66E-05	4.02	-4.62E-10	8.99
	800	1.33E-06	4.01	6.02E-08	4.51	4.15E-06	4.01	-9.03E-13	9.00
	1600	8.29E-08	4.00	2.66E-09	4.50	2.59E-07	4.00	$\sim 10^{-16}$	-
RK(7,4,11)	100	2.92E-03		3.72E-04		8.94E-03		-8.13E-07	
	200	1.74E-04	4.07	1.58E-05	4.56	5.39E-04	4.05	-4.09E-10	10.96
	400	1.07E-05	4.02	6.88E-07	4.52	3.34E-05	4.01	-2.03E-13	10.97
	800	6.68E-07	4.01	3.03E-08	4.51	2.08E-06	4.00	$\sim 10^{-16}$	-
	1600	4.17E-08	4.00	1.34E-09	4.50	1.30E-07	4.00	$\sim 10^{-16}$	-

Let $U = (u_1, u_2, \dots, u_{N_x})^T$, and assuming ρ is constant, we can write the semi-discretized equation in matrix form:

$$U_{tt} = -AU + B, \quad (40)$$

where

$$B = \frac{1}{\rho} (b(x_1, t), \dots, b(x_{N_x}, t))^T, \quad (41)$$

and the entries of the matrix A is defined by

$$A_{ij} = \begin{cases} -\frac{\Delta x}{\rho} C(x_j - x_i), & i \neq j, \\ \frac{\Delta x}{\rho} \sum_{k \neq i} C(x_k - x_i), & i = j. \end{cases} \quad (42)$$

System (40) can be written as a system of first-order equations:

$$\frac{\partial}{\partial t} U = V, \quad (43)$$

$$\frac{\partial}{\partial t} V = -AU + B, \quad (44)$$

and in its matrix form, we have:

$$\frac{\partial}{\partial t} \begin{pmatrix} U \\ V \end{pmatrix} = \begin{pmatrix} 0 & I \\ -A & 0 \end{pmatrix} \begin{pmatrix} U \\ V \end{pmatrix} + \begin{pmatrix} 0 \\ B \end{pmatrix}. \quad (45)$$

The total energy (Hamiltonian) of the system is:

$$\mathcal{E} = \frac{1}{2} V^T V + \frac{1}{2} U^T A U - U^T B. \quad (46)$$

Table 5: Comparison of several fourth-order RK methods for harmonic oscillator simulations.

method	N_t	L_2 error norm	energy error	CPU time (seconds)
RK(4,4,5)	1600	4.24E-08	-3.47E-07	0.073
RK(5,4,7)	800	1.61E-07	-4.63E-09	0.045
RK(6,4,9)	800	6.02E-08	-4.62E-10	0.054
RK(7,4,11)	800	3.03E-08	$\sim 10^{-16}$	0.060

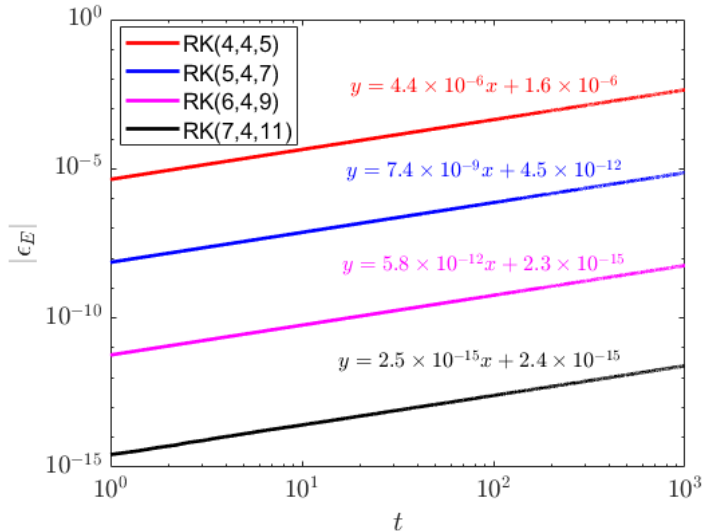


Figure 3: Time history plots (in log-log scale) of the magnitudes of relative energy deviation for harmonic oscillator simulations. The equations represent the linear fitting of the corresponding curve in the same color. Each simulation runs for 5000 steps until $T = 10^3$.

In our simulations, we set $b = 0$, $\rho = 1$, and $\delta = 5$. The computational domain is $x \in [-20, 20]$ and $t \in [0, T]$. We let $\Delta t = \Delta x$. The initial condition is $u(x, 0) = \exp(-x^2)$ and $u_t(x, 0) = 0$. Similar to previous studies [10, 11], a periodic boundary condition is implemented to approximate the original problem of an infinitely long bar. The simulation run until $T = 5$ so that it stops before the solution reaches the boundaries. The exact solution is given by [12]:

$$u_e(x, t) = \frac{2}{\sqrt{\pi}} \int_0^\infty e^{-\xi^2} \cos(2x\xi) \cos\left(2t\sqrt{1 - e^{-\xi^2}}\right) d\xi. \quad (47)$$

The solutions at two time snapshots using the seven-stage method RK(7,4,11) are shown in Figure 4. Results on convergence rates are presented in Table 6. All methods provide fourth-order accurate solutions, but the accuracy improves with larger s due to better energy accuracy.

A comparison of computational cost is illustrated in Table 7, where the seven-stage method RK(7,4,11) demonstrates greater efficiency than the four-stage RK(4,4,5). The RK(7,4,11) method achieves a smaller error with half the mesh size and runs more than four times faster than RK(4,4,5). Additionally, the total energy of the RK(7,4,11) solution reaches machine precision at the final time when $N_x = 800$. The solution to peridynamic equations involves the evaluation of an integral every iteration, so doubling the mesh significantly increases the computational cost in terms of both memory and CPU run time.

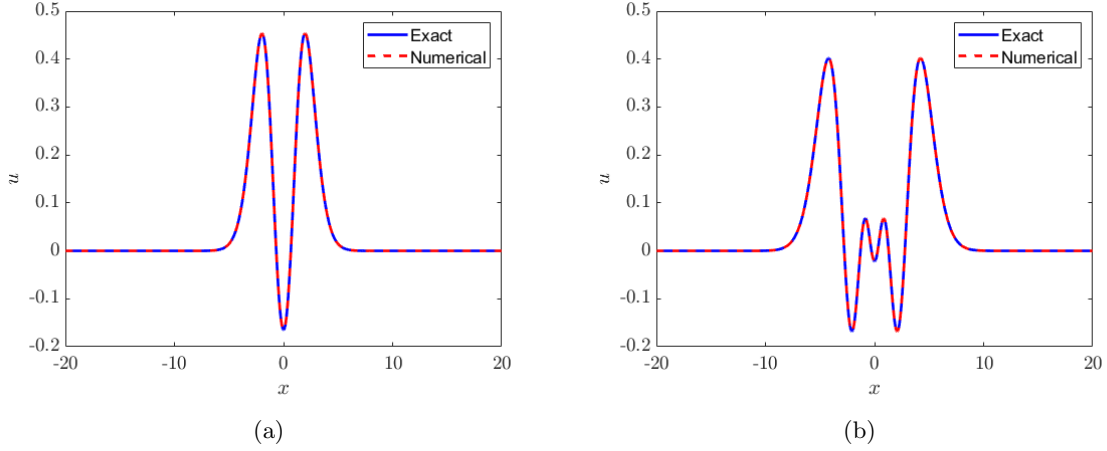


Figure 4: Solutions of the linear peridynamic equation at (a) $t = 2.5$ and (b) $t = 5$ using RK(7,4,11).

3.3 One-dimensional Maxwell's equations

Consider the one-dimensional Maxwell's equations

$$\epsilon_0 \frac{\partial E_z}{\partial t} = \frac{\partial H_y}{\partial x}, \quad (48)$$

$$\mu_0 \frac{\partial H_y}{\partial t} = \frac{\partial E_z}{\partial x}. \quad (49)$$

By employing a staggered grid and centered difference algorithm, we define $E_j^n = E_z(j\Delta x, n\Delta t)$ and $H_{j+1/2}^n = H_y((j+1/2)\Delta x, n\Delta t)$, yielding the semi-discrete equations:

$$\epsilon_0 \frac{\partial}{\partial t} E_z(t_n, x_j) = \frac{H_{j+1/2}^n - H_{j-1/2}^n}{\Delta x}, \quad (50)$$

$$\mu_0 \frac{\partial}{\partial t} H_y(t_n, x_{j+1/2}) = \frac{E_{j+1}^n - E_j^n}{\Delta x}. \quad (51)$$

These equations can be written in matrix form as:

$$\frac{\partial}{\partial t} \begin{pmatrix} \vec{E} \\ \vec{H} \end{pmatrix} = \begin{pmatrix} 1/\epsilon_0 & 0 \\ 0 & 1/\mu_0 \end{pmatrix} \begin{pmatrix} 0 & C \\ -C^T & 0 \end{pmatrix} \begin{pmatrix} \vec{E} \\ \vec{H} \end{pmatrix}, \quad (52)$$

where matrix C represent the finite difference curl operator, and $\vec{E}^n = (E_0^n, E_1^n, \dots, E_N^n)^T$ and $\vec{H}^n = (H_{1/2}^n, H_{3/2}^n, \dots, H_{N+1/2}^n)^T$ are the solution vectors at time $n\Delta t$. For perfect electric conductor (PEC) boundaries, we have $E_0^n = E_N^n = 0$. $H_{N+1/2}^n$ is outside the boundary and is set to zero. For example, when $N_x = 4$, we have:

$$C = \frac{1}{\Delta x} \begin{pmatrix} 1 & 0 & 0 & 0 & 0 \\ -1 & 1 & 0 & 0 & 0 \\ 0 & -1 & 1 & 0 & 0 \\ 0 & 0 & -1 & 1 & 0 \\ 0 & 0 & 0 & -1 & 1 \end{pmatrix}. \quad (53)$$

It can be verified that $\rho(C^T C) \leq \frac{4}{\Delta x^2}$ where ρ stands for the spectral radius of a matrix. Thus, we have:

$$\left\| \begin{pmatrix} 0 & C \\ -C^T & 0 \end{pmatrix} \right\| = \sqrt{\rho(C^T C)} \leq \frac{2}{\Delta x}. \quad (54)$$

Table 6: Solution and energy convergence rates of peridynamic integro-differential equations using fourth-order methods.

Method	N_x	ϵ_1	Order	ϵ_2	Order	ϵ_∞	Order	ϵ_E	Order
RK(4,4,5)	100	2.62E-04	-	5.70E-05	-	2.05E-03	-	-5.86E-03	-
	200	1.58E-05	4.05	2.47E-06	4.53	1.26E-04	4.03	-1.85E-04	4.99
	400	9.63E-07	4.04	1.05E-07	4.56	7.52E-06	4.06	-5.84E-06	4.98
	800	5.93E-08	4.02	4.53E-09	4.53	4.62E-07	4.02	-1.83E-07	5.00
	1600	3.67E-09	4.01	1.98E-10	4.52	2.87E-08	4.01	-5.72E-09	5.00
RK(5,4,7)	100	4.42E-05	-	9.47E-06	-	3.37E-04	-	-1.08E-04	-
	200	2.59E-06	4.09	3.94E-07	4.59	2.02E-05	4.06	-8.32E-07	7.01
	400	1.57E-07	4.05	1.69E-08	4.54	1.22E-06	4.05	-6.55E-09	6.99
	800	9.75E-09	4.01	7.41E-10	4.51	7.60E-08	4.00	-5.12E-11	7.00
	1600	6.08E-10	4.00	3.27E-11	4.50	4.74E-09	4.00	-4.00E-13	7.00
RK(6,4,9)	100	1.53E-05	-	3.27E-06	-	1.20E-04	-	-9.68E-07	-
	200	9.51E-07	4.01	1.44E-07	4.51	7.38E-06	4.02	-1.86E-09	9.02
	400	5.86E-08	4.02	6.30E-09	4.51	4.54E-07	4.02	-3.66E-12	8.99
	800	3.65E-09	4.00	2.78E-10	4.50	2.84E-08	4.00	-7.55E-15	8.92
	1600	2.28E-10	4.00	1.23E-11	4.50	1.77E-09	4.00	$\sim 10^{-16}$	-
RK(7,4,11)	100	7.54E-06	-	1.61E-06	-	5.88E-05	-	-5.06E-09	-
	200	4.76E-07	3.99	7.20E-08	4.48	3.69E-06	3.99	-2.43E-12	11.02
	400	2.94E-08	4.02	3.16E-09	4.51	2.28E-07	4.02	-1.11E-15	11.10
	800	1.84E-09	4.00	1.40E-10	4.50	1.43E-08	4.00	$\sim 10^{-16}$	-
	1600	1.15E-10	4.00	6.18E-12	4.50	8.89E-10	4.01	$\sim 10^{-16}$	-

For the fourth-order RK methods in this work, the corresponding stability condition becomes $\Delta t \leq \frac{\lambda \Delta x}{2c}$, where $c = 1/\sqrt{\epsilon_0 \mu_0}$ is the speed of light and λ is given in Table 2.

The total energy of the system is given by

$$\mathcal{E} = \frac{1}{2} \left(\epsilon_0 \|\vec{E}^n\|^2 + \mu_0 \|\vec{H}^n\|^2 \right). \quad (55)$$

Note that if we define the magnetic field at time $(n + 1/2)\Delta t$, and discretize the equations (50)-(51) using the leapfrog algorithm, we obtained the standard Yee Finite-Difference Time-Domain (FDTD) method [13, 14, 15]. Different from the energy defined in (55), the FDTD method preserves the following numerical energy:

$$\tilde{\mathcal{E}} = \frac{1}{2} \left(\epsilon_0 \|\vec{E}^n\|^2 + \mu_0 \langle \vec{H}^{n-1/2}, \vec{H}^{n+1/2} \rangle \right). \quad (56)$$

In our simulations, the computational domain covers $x \in [-5, 5]$ and $t \in [0, 10^{-8}]$ with PEC boundaries. The initial condition is a Gaussian pulse defined as

$$E(0, x) = \phi(x) = e^{-5x^2} \sin\left(\frac{2\pi}{\lambda_0} x\right), \quad (57)$$

with a carrier wavelength of $\lambda_0 = 0.2$. The simulation runs until $T = 10^{-8}$, ensuring it stops before the solution reaches the boundaries. The exact solution is obtained using traveling wave solution: $E(t, x) = 0.5(\phi(x + ct) + \phi(x - ct))$.

The simulation results are summarized in Table 8. All four RK methods exhibit similar accuracy, with convergence rates of the solutions being second-order due to the spatial discretization

Table 7: Comparison of fourth-order RK methods for peridynamic equations.

method	N_x	L_2 error norm	energy error	CPU time (seconds)
RK(4,4,5)	1600	1.98E-10	-5.72E-09	17.40
RK(5,4,7)	800	7.41E-10	-5.12E-11	2.77
RK(6,4,9)	800	2.78E-10	-3.66E-12	3.30
RK(7,4,11)	800	1.40E-10	$\sim 10^{-16}$	3.66

being second-order. To assess computational efficiency, we compare against the FDTD method. For FDTD, we choose a Courant number of 1, so $\Delta t = \frac{\Delta x}{c}$. As shown in Table 9, the fourth-order RK methods achieve better accuracy and run faster than the fine mesh FDTD result. The RK methods do not significantly increase the computational cost, partly because they use larger Δt (equivalently, smaller N_t). In this simulation, both the six- and seven-stage methods achieve energy accuracy of machine precision at the final time when the grid size is $N_x = 16,000$.

To compare the energy dissipation over a long time, we run the simulations for 100,000 iterations with the same Courant number of 0.5 ($\Delta t = 0.5 \frac{\Delta x}{c}$) for all methods. The computational mesh size is fixed at $N_x = 1000$, resulting in a resolution of 20 cells per wavelength ($\Delta x = \frac{\lambda_0}{20}$). The results are shown in Figure 5. At the end of the simulation ($n_t = 100,000$), the energy dissipation decreases by approximately 3 orders of magnitude as s increases by one. Specifically, the energy dissipation of the RK(4,4,5) method is about 0.02, compared to 4.7×10^{-12} for the RK(7,4,11) method. This demonstrates that the energy accuracy can be significantly enhanced by employing superconvergent methods.

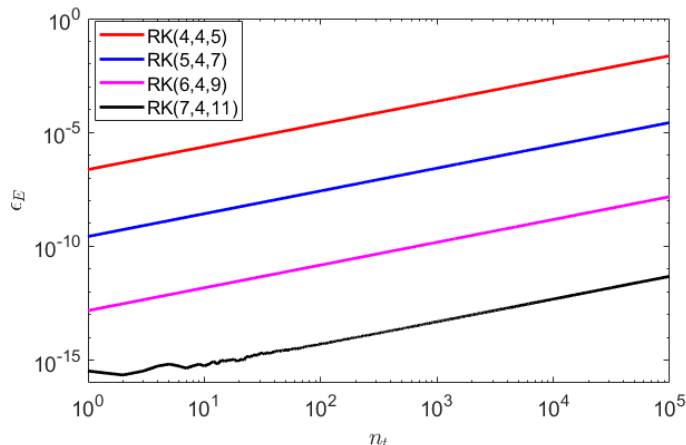


Figure 5: Time history plots (in log-log scale) of the magnitude of the relative energy deviation for the solution to 1D Maxwell’s equations using several fourth-order RK methods. $\Delta x = \frac{\lambda_0}{20}$. The Courant number is fixed at 0.5. Each simulation runs for 100,000 iterations.

4 Conclusion

Through the study of energy convergence rates of explicit Runge-Kutta (RK) methods for antisymmetric linear autonomous systems, we have developed a class of energy-superconvergent RK methods in which the orders of energy accuracy exceed the number of stages. For an s -stage RK method of an even order p , the energy accuracy can achieve up to an order of $2s - p + 1$. Generally, higher order energy accuracy leads to a larger stability region and thus a larger step

Table 8: Solution and energy convergence rates for 1D Maxwell’s equations using fourth-order RK methods.

Method	N_x	ϵ_1	Order	ϵ_2	Order	ϵ_∞	Order	ϵ_E	Order
RK(4,4,5)	2000	3.8414E-03		2.3641E-04		5.2370E-02		-8.07E-04	
	4000	9.4638E-04	2.02	4.1187E-05	2.52	1.2910E-02	2.02	-2.55E-05	4.98
	8000	2.3568E-04	2.01	7.2527E-06	2.51	3.2140E-03	2.01	-7.99E-07	5.00
	16000	5.8863E-05	2.00	1.2809E-06	2.50	8.0279E-04	2.00	-2.50E-08	5.00
	32000	1.4712E-05	2.00	2.2638E-07	2.50	2.0064E-04	2.00	-7.81E-10	5.00
RK(5,4,7)	2000	3.7922E-03		2.3330E-04		5.1708E-02		-7.72E-06	
	4000	9.4262E-04	2.01	4.1024E-05	2.51	1.2851E-02	2.01	-6.11E-08	6.98
	8000	2.3551E-04	2.00	7.2475E-06	2.50	3.2120E-03	2.00	-4.79E-10	6.99
	16000	5.8839E-05	2.00	1.2803E-06	2.50	8.0245E-04	2.00	-3.74E-12	7.00
	32000	1.4711E-05	2.00	2.2636E-07	2.50	2.0063E-04	2.00	-3.16E-14	6.89
RK(6,4,9)	2000	3.7854E-03		2.3286E-04		5.1611E-02		-3.55E-08	
	4000	9.4187E-04	2.01	4.0992E-05	2.51	1.2837E-02	2.01	-7.03E-11	8.98
	8000	2.3531E-04	2.00	7.2414E-06	2.50	3.2092E-03	2.00	-1.39E-13	8.99
	16000	5.8843E-05	2.00	1.2804E-06	2.50	8.0249E-04	2.00	$\sim 10^{-16}$	-
	32000	1.4711E-05	2.00	2.2635E-07	2.50	2.0062E-04	2.00	$\sim 10^{-16}$	-
RK(7,4,11)	2000	3.7724E-03		2.3225E-04		5.1375E-02		-6.12E-11	
	4000	9.4246E-04	2.00	4.1015E-05	2.50	1.2854E-02	2.00	-3.01E-14	10.99
	8000	2.3534E-04	2.00	7.2423E-06	2.50	3.2098E-03	2.00	$\sim 10^{-16}$	-
	16000	5.8833E-05	2.00	1.2802E-06	2.50	8.0237E-04	2.00	$\sim 10^{-16}$	-
	32000	1.4711E-05	2.00	2.2636E-07	2.50	2.0063E-04	2.00	$\sim 10^{-16}$	-

size. Additionally, we have derived the strong stability criteria for several fourth-order methods when $5 \leq s \leq 7$. We present numerical solutions of ODEs for harmonic oscillators and nonlocal integro-differential equations for peridynamics, demonstrating that the energy error can reach machine precision for methods with higher-order energy accuracy. When comparing methods with the same solution orders but different energy accuracy, the error due to time discretization decreases as the order of energy accuracy increases. A method with higher-order energy accuracy exhibits comparable computational efficiency to lower-order ones. Furthermore, the proposed RK methods are used as the time discretization method for the semi-discretized one-dimensional Maxwell’s equations on a spatially staggered grid, similar to the Yee FDTD method. While the RK-based methods maintain second-order accuracy due to spatial discretization, they offer superior accuracy and permit larger time steps than the FDTD method, leading to better efficiency.

References

- [1] Doron Levy and Eitan Tadmor. From semidiscrete to fully discrete: Stability of runge–kutta schemes by the energy method. *SIAM review*, 40(1):40–73, 1998.
- [2] Sigal Gottlieb and Chi-Wang Shu. Total variation diminishing runge-kutta schemes. *Mathematics of computation*, 67(221):73–85, 1998.
- [3] Sigal Gottlieb, Chi-Wang Shu, and Eitan Tadmor. Strong stability-preserving high-order time discretization methods. *SIAM review*, 43(1):89–112, 2001.

Table 9: Comparison of FDTD and fourth-order RK methods for 1D Maxwell’s equations.

method	N_x	N_t	$c \frac{\Delta t}{\Delta x}$	ϵ_1	ϵ_2	ϵ_∞	ϵ_E	CPU time (seconds)
FDTD	32000	9593	1.0	1.76E-04	2.74E-06	2.45E-03	$\sim 10^{-16}$	2.09
RK(4,4,5)	16000	3392	$\sqrt{2}$	5.88E-05	1.28E-06	8.02E-04	-2.50E-08	1.31
RK(5,4,7)	16000	2769	$\sqrt{3}$	5.88E-05	1.28E-06	8.02E-04	-3.74E-12	1.32
RK(6,4,9)	16000	2477	$\frac{\sqrt{15}}{2}$	5.88E-05	1.28E-06	8.02E-04	$\sim 10^{-16}$	1.39
RK(7,4,11)	16000	2398	2.0	5.88E-05	1.28E-06	8.02E-04	$\sim 10^{-16}$	1.54

- [4] Eitan Tadmor. From semidiscrete to fully discrete: stability of runge-kutta schemes by the energy method. ii. *Collected lectures on the preservation of stability under discretization*, 109:25–49, 2002.
- [5] Zheng Sun and Chi-Wang Shu. Stability of the fourth order runge–kutta method for time-dependent partial differential equations. *Annals of Mathematical Sciences and Applications*, 2(2):255–284, 2017.
- [6] Zheng Sun and Chi-Wang Shu. Strong stability of explicit runge–kutta time discretizations. *SIAM Journal on Numerical Analysis*, 57(3):1158–1182, 2019.
- [7] Bernardo Cockburn and Chi-Wang Shu. Runge–kutta discontinuous galerkin methods for convection-dominated problems. *Journal of scientific computing*, 16:173–261, 2001.
- [8] Stewart A Silling. Reformulation of elasticity theory for discontinuities and long-range forces. *Journal of the Mechanics and Physics of Solids*, 48(1):175–209, 2000.
- [9] Ernst Hairer, Christian Lubich, and Gerhard Wanner. Geometric numerical integration illustrated by the störmer–verlet method. *Acta numerica*, 12:399–450, 2003.
- [10] Giuseppe Maria Coclite, Alessandro Fanizzi, Luciano Lopez, Francesco Maddalena, and Sabrina Francesca Pellegrino. Numerical methods for the nonlocal wave equation of the peridynamics. *Applied Numerical Mathematics*, 155:119–139, 2020.
- [11] Jinjie Liu, Samuel Appiah-Adjei, and Moysey Brio. Iterated crank–nicolson method for peridynamic models. *Dynamics*, 4(1):192–207, 2024.
- [12] Olaf Weckner and Rohan Abeyaratne. The effect of long-range forces on the dynamics of a bar. *Journal of the Mechanics and Physics of Solids*, 53(3):705–728, 2005.
- [13] Kane Yee. Numerical solution of initial boundary value problems involving maxwell’s equations in isotropic media. *IEEE Transactions on antennas and propagation*, 14(3):302–307, 1966.
- [14] A. Taflove and M. E. Brodwin. Numerical solution of steady-state electromagnetic scattering problems using the time-dependent Maxwell’s equations. *IEEE Trans. Microwave Theory Tech.*, 23:623–630, 1975.
- [15] A. Taflove and S. Hagness. *Computational Electrodynamics: The Finite-Difference Time-Domain Method*. Artech House, Norwood, MA, 3rd edition, 2005.